Escape of ionising photons from star-forming regions in nearby galaxies

Mónica Relaño Pastor

University of Granada

Escape of Lyman radiation from galactic labyrinths, 11-14 September 2018, OAC, Kolymbari, Crete

Density-bounded HII regions

- OB associations ionised the ISM around them and create a region of ionised gas.

$$N_* = \int_{\nu_o}^{\infty} \frac{L_\nu}{h\nu} = \frac{4}{3}\pi R_S^3 N_H^2 \alpha_B$$

Ionisation bounded nebula

Nakajima & Ouchi 2014

Density-bounded HII regions

- OB associations ionised the ISM around them and create a region of ionised gas.

$$N_* = \int_{\nu_o}^{\infty} \frac{L_\nu}{h\nu} = \frac{4}{3}\pi R_S^3 N_H^2 \alpha_B$$

Ionisation bounded nebula

Not enough gas to absorb all the ionising flux

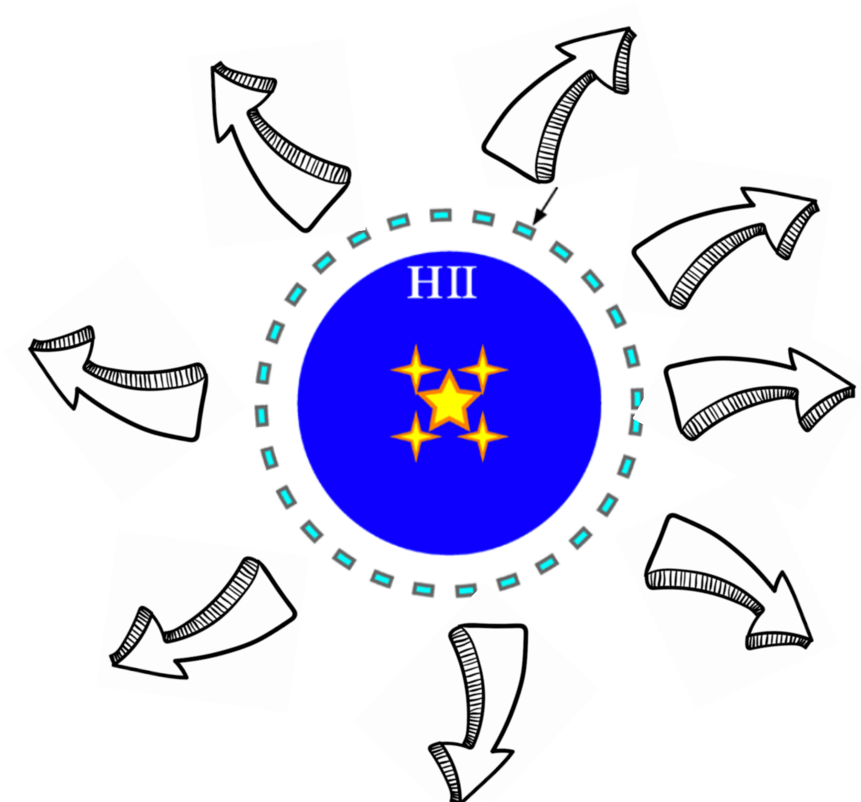

Density bounded nebula

Nakajima & Ouchi 2014

Measuring leakage of ionising radiation

Stellar content:

- Comparison of the ionising radiation coming from the stars with the HII region luminosity.
- Spectral classification of the stars (early type stars contribute ≈ 90% of the ionising flux)
- $Q(H^{\circ}) = 2.2\, Q(H\alpha)$, under T_e= 10000K and Case B

Limitations:

- Only in LMC/SMC HII regions (e.g. NGC 300 is far away, but see Roth et al. 2018 and Eldridge & Relaño 2012 for NGC 604 in M33)
- Requires spectroscopic observations: broad-band observations do not give accurate spectral classification (see Niederhorfer et al. 2016 for regions in NGC 300)
- Different $Q(H^{\circ})$ depending on the stellar atmosphere model assumptions and metallicity (Oey & Kennicutt 1997, Voges et al. 2008)
- Stellar population including binaries can increase the ionising flux by 60% at low metallicities and 10-20% at near-Solar metallicity (Stanway et al. 2016) and can predict older ages (~10Myr) for the HII regions compared to (~5Myr) single star models (Xiao et al. 2018).

Stellar content

Observed and predicted HII region luminosities in LMC

H II Region	L_{obs} (erg s^{-1})	L_P (erg s^{-1})	L_{VGS} (erg s^{-1})	L_{SdK} (erg s^{-1})	$Q(H^0)$ (s^{-1})	$n_\star$	$E(B-V)$ (mag)	L_{obs}/L_{SdK}
DEM 10B	6.68E+37	5.33E+37	9.61E+37	8.24E+37	8.64E+49	7	0.16	0.81
DEM 25	2.64E+37	2.23E+36	3.88E+36	3.08E+36	2.88E+48	1	0.11	8.57
DEM 31	6.42E+37	1.11E+38	1.73E+38	1.62E+38	1.45E+50	6	0.09	0.40
DEM 34	5.46E+38	6.83E+38	9.37E+38	8.33E+38	7.61E+50	44*	0.10	0.66
DEM 50	4.61E+37	1.61E+37	2.70E+37	2.30E+37	2.20E+49	3	0.12	2.00
DEM 106	3.43E+37	4.15E+37	7.34E+37	5.55E+37	5.56E+49	8	0.14	0.61
DEM 152+156[a]	2.32E+38	3.18E+38	4.11E+38	3.52E+38	3.22E+50	35*	0.10	0.66
DEM 192	2.50E+38	2.61E+38	3.66E+38	3.03E+38	2.71E+50	25*	0.09	0.83
DEM 199	4.09E+38	3.00E+38	3.94E+38	3.34E+38	2.72E+50	22*	0.05	1.22
DEM 226	2.23E+37	1.65E+37	2.85E+37	2.41E+37	2.53E+49	4	0.16	0.93
DEM 243	5.22E+37	6.14E+37	1.19E+38	9.72E+37	8.88E+49	11	0.10	0.54
DEM 293	4.97E+37	8.11E+37	4.78E+37	4.56E+37	4.79E+49	1	0.16	1.09
DEM 301	4.84E+37	1.87E+38	2.65E+38	2.45E+38	2.04E+50	7	0.06	0.20
DEM 323+326	3.30E+38	3.88E+38	3.24E+38	2.92E+38	2.80E+50	20	0.12	1.13

* WR star excluded; DEM 199 contains three WR stars.
[a]Not including DEM 152A.

(WR and B stars not included)

Oey & Kennicutt 1997

$$\frac{L(H\alpha)_{obs}}{L_{SdK}} \sim 0.74$$

Ionising radiation is leaking from the HII regions in the sample

$$f_{esc} \sim 0 - 51\ \%$$

- Superbubbles have lower ratios (holes that allow the ionising radiation to escape the region).
- DEM 25 and DEM 50 show evidence of recent supernova activity

Stellar content

Voges et al. 2008 revisited Oey & Kennicutt 1997 results with updated (MSH, SNC) stellar atmosphere models.
Add 39 more HII regions (spectral type from broadband UBVR observations)

Voges et al. 2008

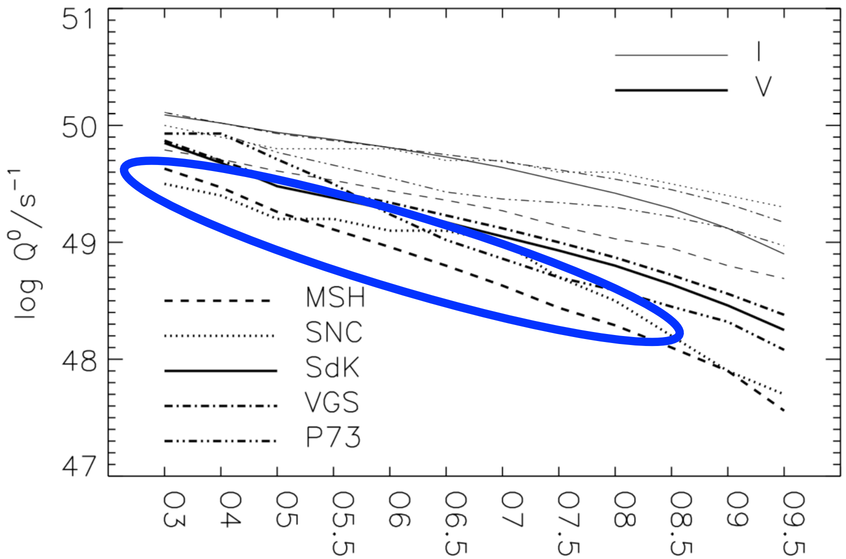

- SNC and MSH models predict softer ionising SEDs than previous studies.

$$f_{esc} \sim 20 - 30\,\%$$

Density bounded HII regions have typically shell like morphology

MSH: Martins et al. 2005, SNC: Smith et al. 2002, SdK: Schaerer & de Koter 1997, VGS: Vacca et al. 1996, and P73: Panagia 1973. All models are at $Z_{\odot}$.

Stellar content

Blue (XMM-Newton), green ([OIII] 501.1nm, NTT), red 8µm, Spitzer, Gouliermis et al. 2008

Most luminous HII region in SMC

- well-studied stellar content (Massey et al. 1989, Gouliermis et al. 2006, Evans et al. 2006)
- New star formation triggered by the wind-driven expanding bubble (Gouliermis et al. 2008)
- Relaño et al. 2002: 58 stars within the region (33 with spectral type classification and one binary)
- Different stellar models at $Z_* = Z_\odot$ and $Z_* = 0.2\ Z_\odot$ gives:

$$f_{esc} \sim 45 \pm 15\ \%$$

Measuring leakage of ionising radiation

Emission line ratios:

- Low ionisation species ([OII], [OI], [SII]) dominate the outer parts of the ionisation bounded regions while they are *suppressed* in density bounded objects.
- 1-dimensional emission line ratios (e.g Castellanos et al. 2002, Iglesias-Páramo et al. 2002, Relaño et al. 2002).
- **I**onisation **P**arameter **M**apping (**IPM**): 2-dimensional mapping of low and high ionisation emission line ratios (e.g. [SII]/[OIII], Pellegrini et al. 2012)

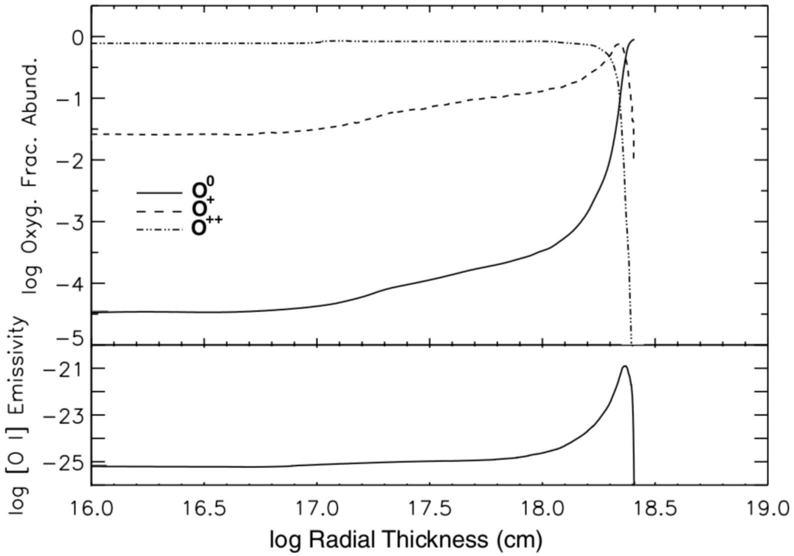

Iglesias-Páramo et al. 2002

Limitations:

- Some emission lines are difficult to detect and can be affected by shocks.
- 1-dimensional emission line ratios does not account for possible irregular morphologies of the regions (partially density-bounded)

Emission line ratios

NGC 346: Ratio involving low ionisation degree emission lines

Models	$I(\lambda6300)/I(H\beta)$	$I(\lambda6717)/I(H\beta)$	$I(\lambda3727)/I(H\beta)$
$Z_* = 0.2Z_\odot$:			
L.1	−5.402	−2.244	−1.008
L.2	−3.155	−1.140	0.049
L.3	−2.953	−1.042	0.135
L.4	−3.340	−1.230	−0.036
L.5	−3.289	−1.279	−0.018
L.6	−3.362	−1.174	−0.052
L.7	−3.609	−1.327	−0.334
Blackbody spectrum:			
B.1	−5.277	−2.136	−0.840
B.2	−3.878	−1.433	−0.174
B.3	−3.328	−1.029	0.288
$Z_* = Z_\odot$:			
S.1	−5.600	−2.297	−1.255
S.2	−3.219	−1.116	−0.109
IL.4 [a]	−2.270	−0.861	0.234
IS.2 [a]	−1.707	−0.844	0.193
Observations[b]	< −2.016	−1.284	−0.040

Lejeune et al. 1997

Schaere & de Kotter (1997)

Relaño et al. 2002

In units of log $I(\lambda_1)/I(\lambda_2)$

Density bounded Models: 1 constant density, 2, 3, 4 different filling factors, 5,6: different gaseous abundance, 7: decreasing density law. **IL: ionisation-bounded models.**

One dimensional ionisation-bounded models cannot reproduce the ratios involving lines with low degree of ionisation: [OI]6300/Hβ, [SII]6717/Hβ, [OII]3727/Hβ (also seen in Castellanos et al. 2002)

Emission line ratios

Ionisation **P**arameter **M**apping **(IPM):** Pellegrini et al. 2012

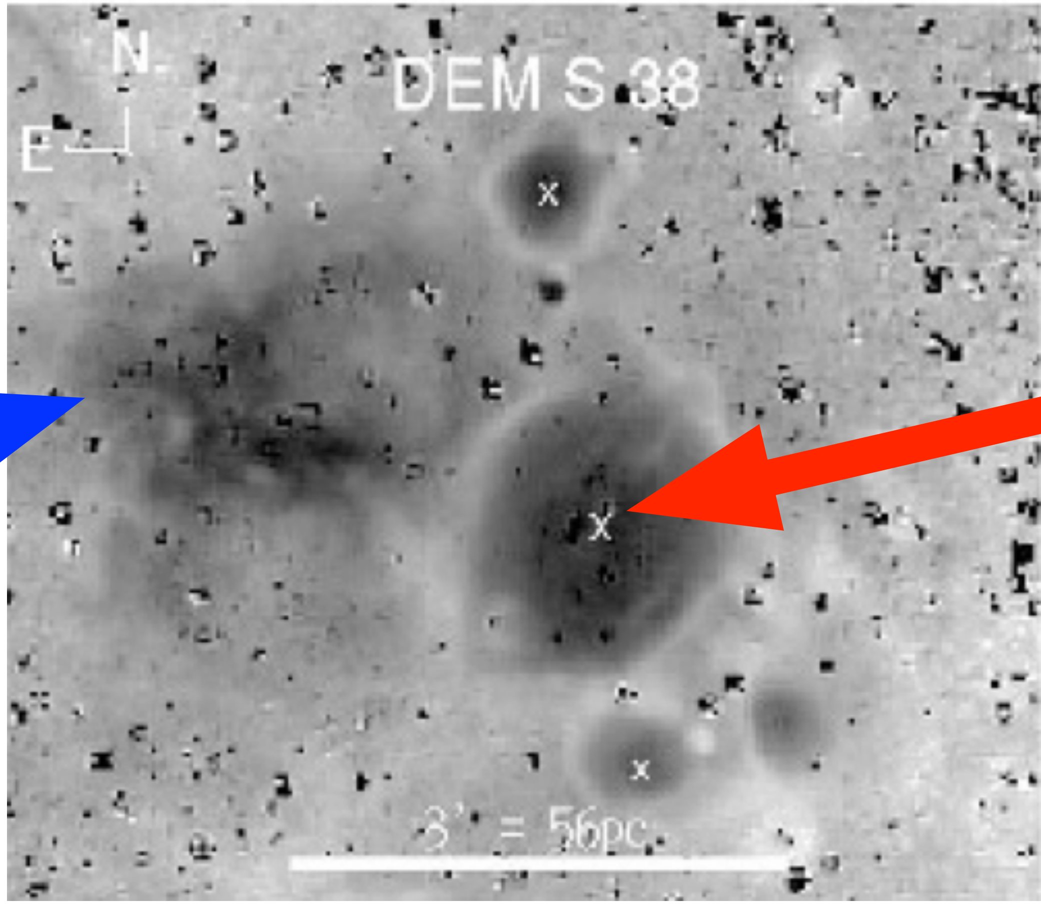

Optically thin: no signature of a transition zone in the gas ionisation state

Optically thick: highly ionised gas surrounded by an ionisation transition zone with higher [SII]/[OIII]

[SII]/[OIII] ratio map: low values are dark, high values are light

Emission line ratios

- Radiation bounded HII regions from Vogel et al (2008) are classified as thick regions by the IPM method.
- Number of optically thin objects is higher for log L(Hα) > 37.0 (in agreement with predictions from Beckman et al. 2000)

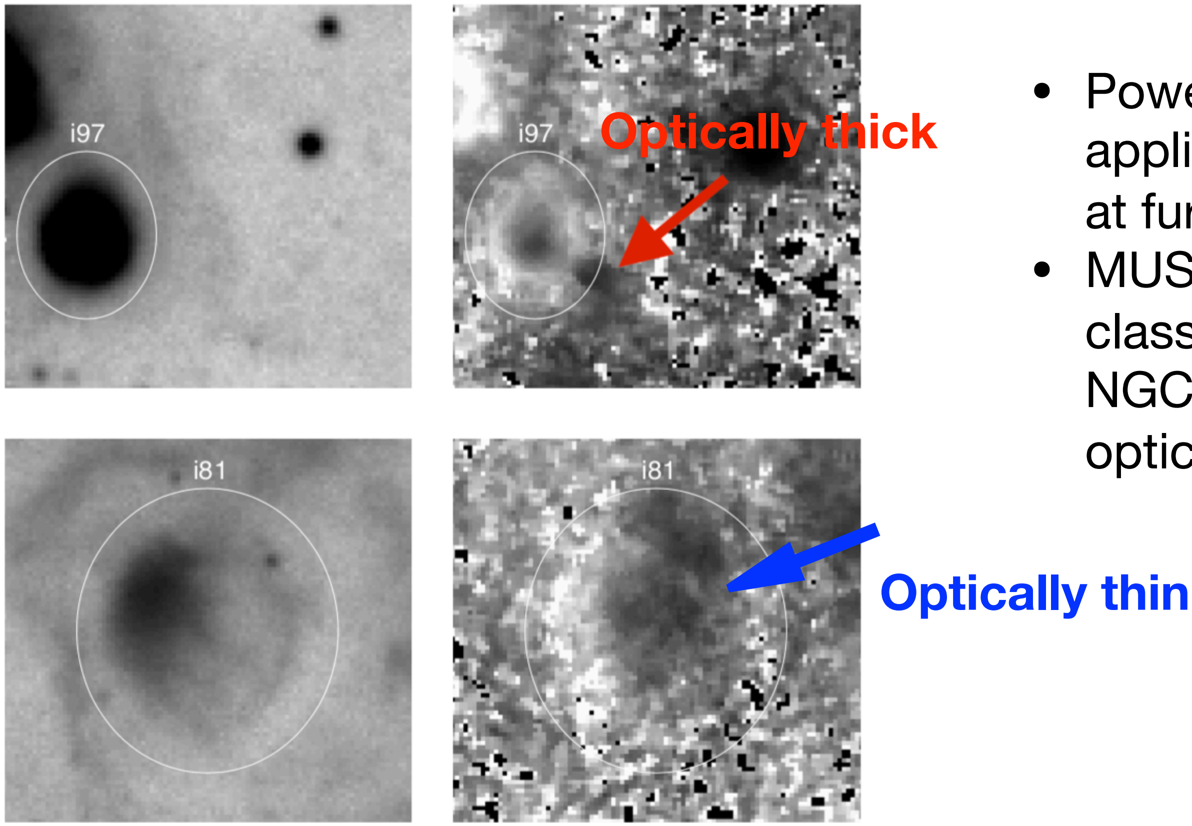

Hα and [SII]/[OIII] maps of two HII regions in NGC 300, Roth et al. 2018

- Powerful method to be applied to HII regions located at further distances
- MUSE observations allow to classified the HII regions of NGC 300 (D=1.9 Mpc) in optically thick and thin objects

Photometric studies

- Change in the slope in the HII luminosity function of spiral galaxies at $L_{Str}=10^{38.6}$ erg s^{-1} (e.g. Knapen et al. 1993, Rozas et al. 1996, 2000, Zurita et al. 2000)

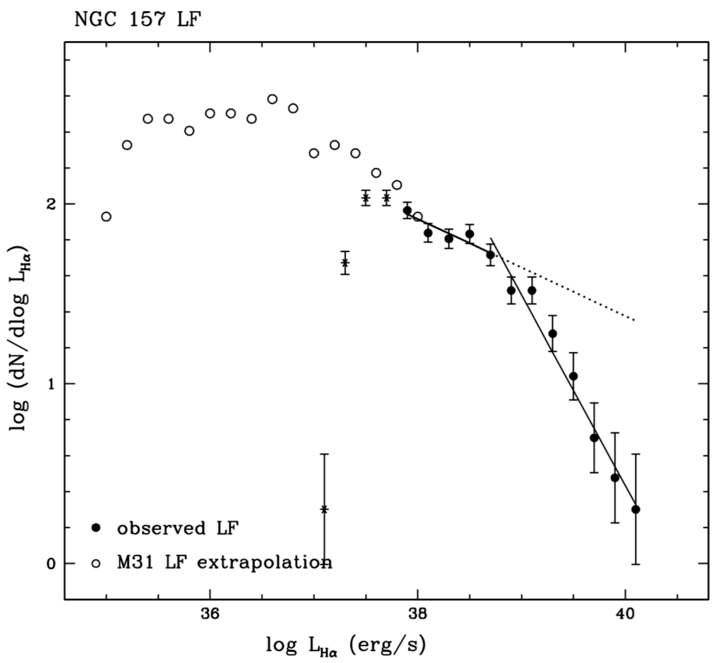

Zurita et al. 2000

- Beckman et al. (2000): Attribute the change to a transition from ionisation to density bounded HII regions.
- The difference between the dotted extrapolation and the solid fit yields the escaping Lyc flux from HII regions.
- The escaping flux exceeds the flux needed to keep the DIG ionised.

Also supported by the IPM in the Magellanic Clouds

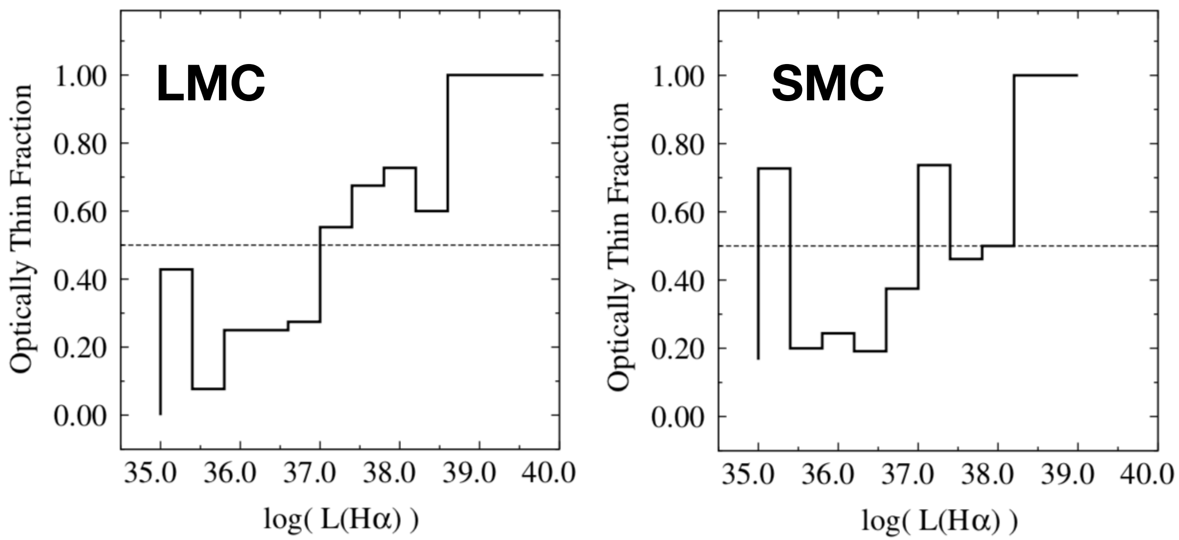

Pellegrini et al. 2012

Where is the ionising radiation going?

- Escape fraction in the LMC of 0-51% is in agreement with L(diffuse)/L(total) ~ 35% (Kennicutt et al. 1995) and for other galaxies (20-50%, Ferguson et al. 1996, Zurita et al. 2002).
- Initial quantitative estimate of the escape fraction of ionising radiation to the IGM (Pellegrini et al. 2012):

$$f_{esc,gal} = \frac{L_{esc} - L_{DIG}}{L_{tot}}$$

$f_{esc,gal} \sim 4-9\,\%$ SMC

$f_{esc,gal} \sim 11-17\,\%$ LMC

- Starbursts (log $\Sigma_{H\alpha}$ > 39.4) show low HI gas fractions and *low* f_{WIM}: evidence of ionising radiation escaping from these galaxies

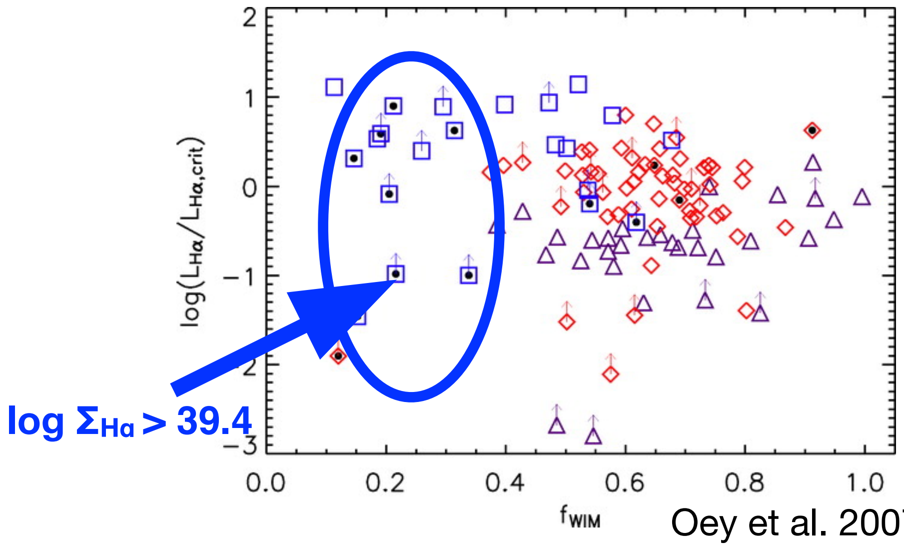

Oey et al. 2007

$L_{H\alpha,crit}$ is a luminosity threshold above which galaxies are expected to release ionising photons and galactic super winds (Clarke & Oey 2002)

f_{WIM}: fraction of diffuse Hα emission defined by the spatial separation between the warm ionised medium and HII regions.

SFR estimations

- Hα nebular emission line emission is a widely used SFR indicator (Kennicutt 1998).
- The Hα emission comes from the recombination of gas ionised by the most massive O- and early-type B-stars
- If there is ionising radiation escaping the HII regions the observed Hα emission does not account for the total SFR within the region.
- *Local* (spatial scale ~500 pc) SFR estimations may be biased downwards by about ~30% of their values (Calzetti 2012)
- For *global* and high SFRs based in large aperture Hα photometry leakage of ionising photons from galaxies is likely negligible at the level of a few percent (e.g. Lee et al. 2009)
- The effects of leakage is more severe in low-mass low-density galaxies.

SFR for low-mass galaxies

11 Mpc Hα UV Galaxy Survey (11HUGS): ~300 star-forming galaxies within 11 Mpc, 80% have Hα-based SFRs < 0.1 $M_\odot$ yr^{-1}

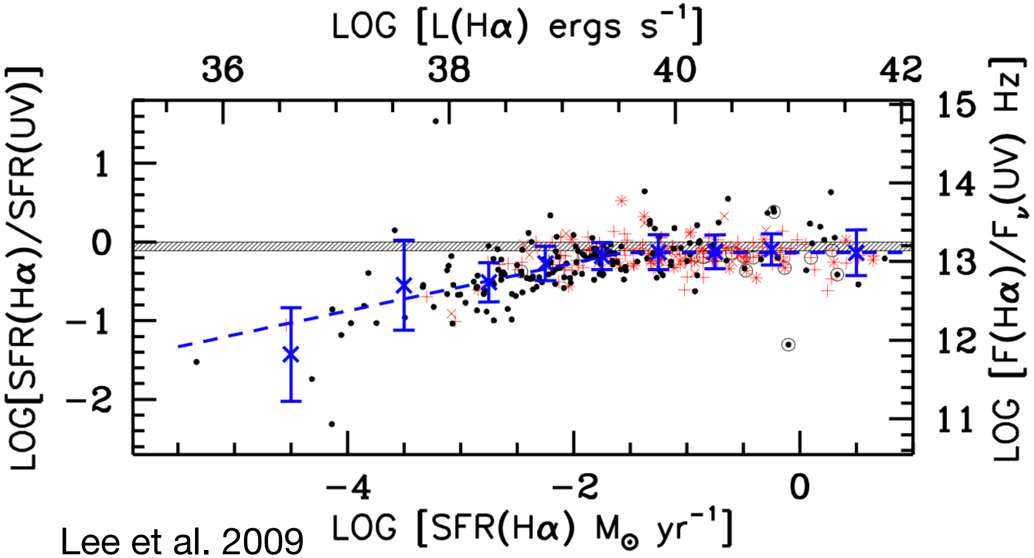

Lee et al. 2009

SFRs obtained following Kennicutt 1998 calibrations (Salpeter IMF, stellar population models with $Z_\odot$, and constant SFR for the last ~100Myr). Extinction corrections applied to both SFR estimations.
For SFR < 0.003 $M_\odot$ yr^{-1} SFR(Hα) is lower than SFR(FUV) by a factor of 2.

SFR(Ha)/SFR(UV) < 1 has been found before in the literature (e.g. Sullivan et al. 2004, Bell & Kennicutt 2001, Meurer et al. 2009, Iglesias-Páramo et al. 2004, etc.)

Possible explanations for the discrepancy (Meurer et al. 2009)**:** Dust absorption, detailed SFH, **porosity of the ISM**, stochasticity of the IMF, metallicity and IMF variations.

Porosity of the ISM

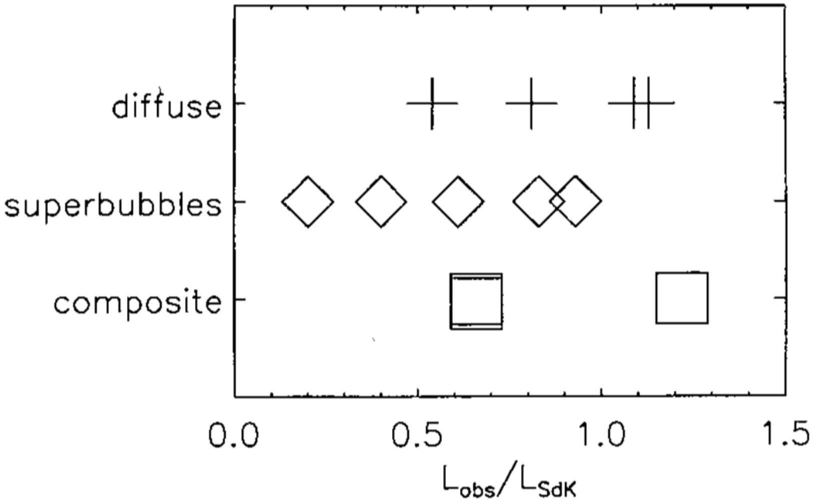

Oey & Kennicutt 1997

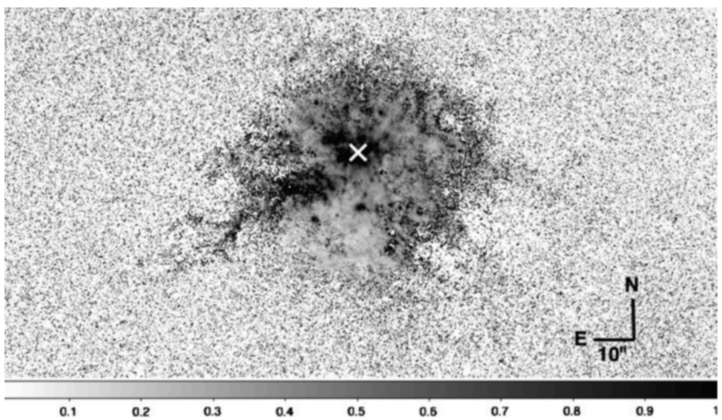

[SIII]/[SII] ratio map for NGC 5253 (Zastrow et al. 2011)

- Superbubbles tend to have lower ratios of observed to predicted Hα luminosities: 0.59 versus 0.89 for diffuse objects (also supported in the revision of this work by Voges et al. 2008).

- Zastrow et al. 2013, 2011: IPM in 7 starburst galaxies shows that axis of escape aligned with the line of sight is a bias for determination of f_{esc}.

- ISM morphology is a critical determinant of whether ionising photons will escape a galaxy

Porosity of the ISM

Morphological classification (*compact, mixed and shells*) of the dwarf galaxies in the sample of Lee et al. 2009, HII regions in LMC and M33 based on Hα emission

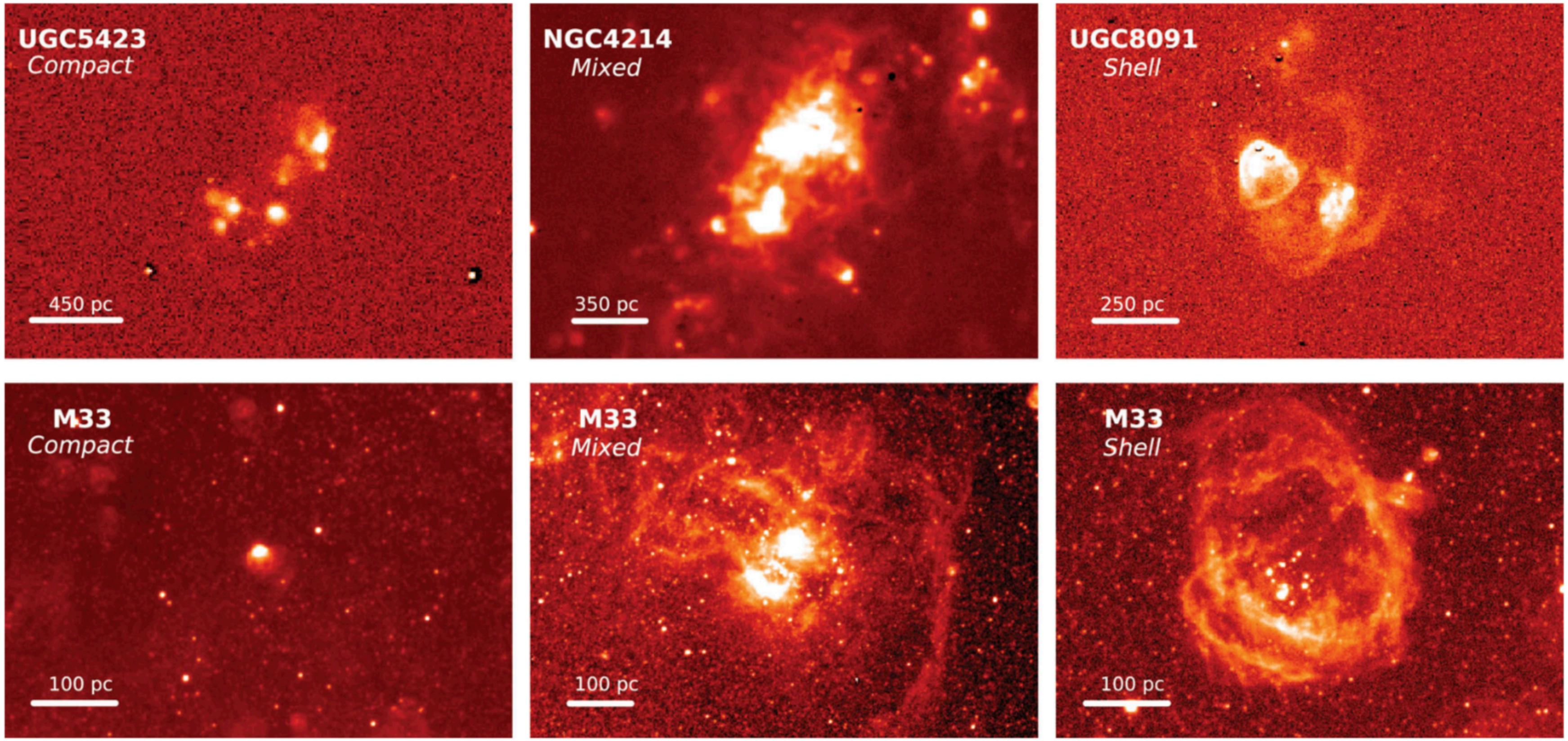

Relaño et al. 2012

Porosity of the ISM

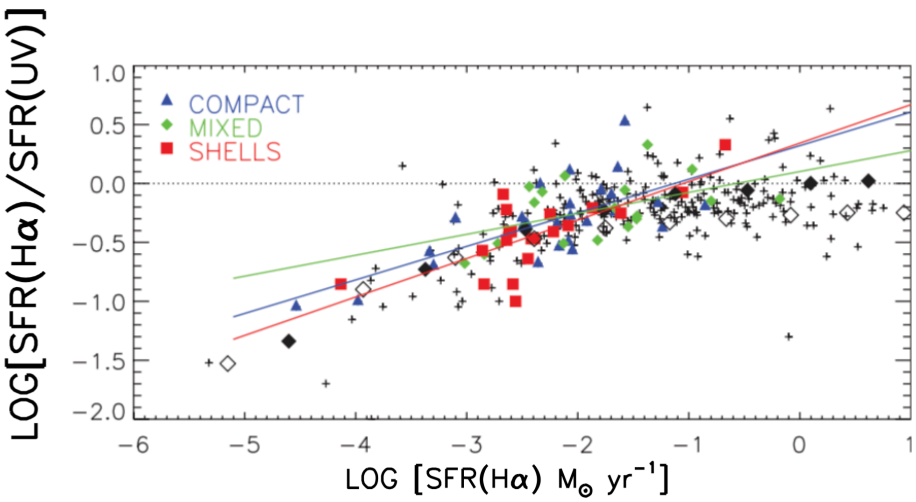

- Extinction correction applied (for Hα using the Balmer decrement and FUV using TIR/FUV ratio)
- Differences in log [SFR(Hα)/SFR(FUV)] for compact and shells of ~1.1-1.4σ
- Maximum differences gives $f_{esc} \sim$ 0-25%

Relaño et al. 2012

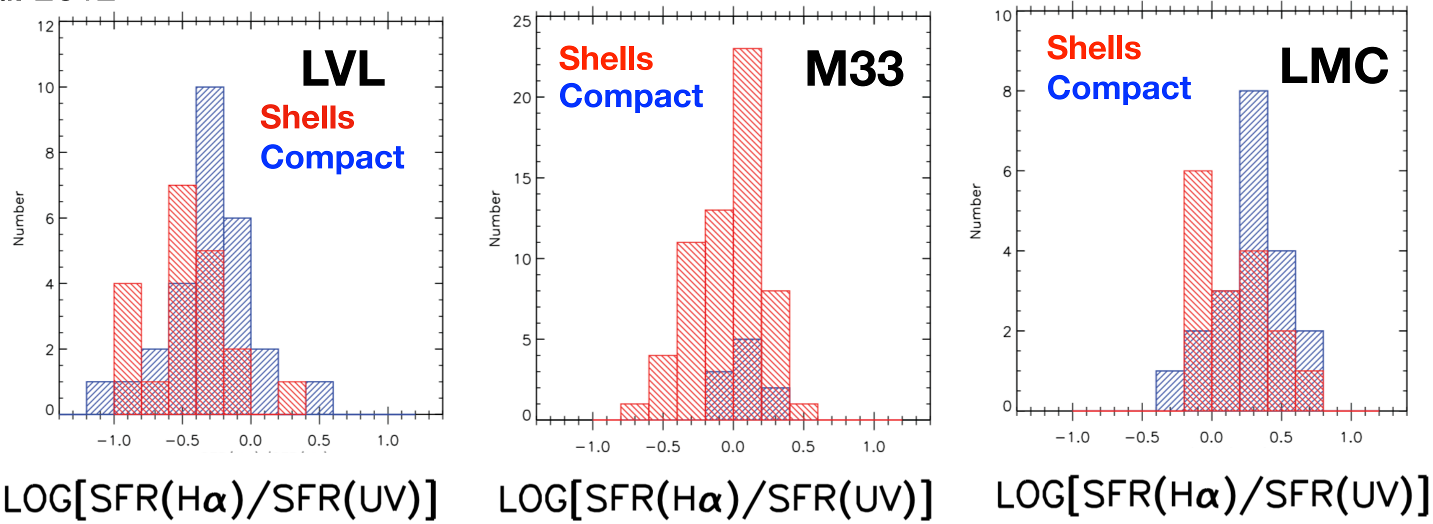

Separation: 0.11 ± 0.10 0.10 ± 0.07 0.12 ± 0.09

Porosity of the ISM

- Shell morphology favours the existence of low-density areas with holes where the ionising photons can escape ==> the difference in log [SFR(Hα)/SFR(FUV)] could be due to leakage of ionising photons, implying f_{esc} ~0-25%

Porosity of the ISM

- Shell morphology favours the existence of low-density areas with holes where the ionising photons can escape ==> the difference in log [SFR(Hα)/SFR(FUV)] could be due to leakage of ionising photons, implying f_{esc} ~0-25%

- Other explanations for the observed SFR(Hα)/SFR(FUV) behaviour:
  - Absorption of LyC photons by the dust inside the regions (Inoue 2001): shells would have higher fractions of dust than compact regions (this is not observed, Verley et al. 2010)

Porosity of the ISM

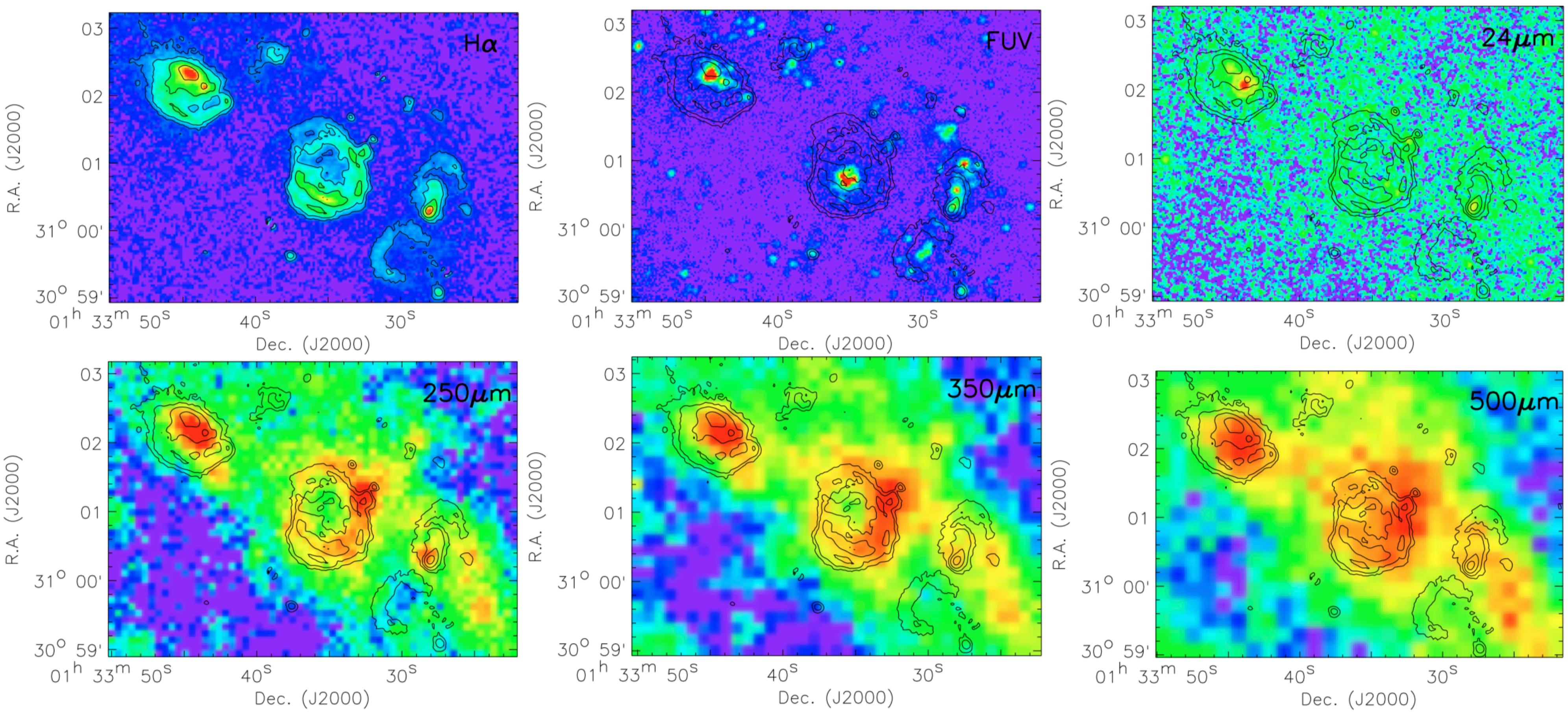

Verley et al. 2010

Porosity of the ISM

- Shell morphology favours the existence of low-density areas with holes where the ionising photons can escape ==> the difference in log [SFR(Hα)/SFR(FUV)] could be due to leakage of ionising photons, implying f_{esc} ~0-25%

- Other explanations for the observed SFR(Hα)/SFR(FUV) behaviour:
  - Absorption of LyC photons by the dust inside the regions (Inoue 2001): shells would have higher fractions of dust than compact regions (this is not observed, Verley et al. 2010)
  - Non-constant SFR: to explain the observed trends very intense (a factor of 100) and very long (~100 Myr) bursts of star formation (Iglesias-Páramo et al. 2004)

Porosity of the ISM

- Shell morphology favours the existence of low-density areas with holes where the ionising photons can escape ==> the difference in log [SFR(Hα)/SFR(FUV)] could be due to leakage of ionising photons, implying f_{esc} ~0-25%

- Other explanations for the observed SFR(Hα)/SFR(FUV) behaviour:
  - Absorption of LyC photons by the dust inside the regions (Inoue 2001): shells would have higher fractions of dust than compact regions (this is not observed, Verley et al. 2010)
  - Non-constant SFR: to explain the observed trends very intense (a factor of 100) and very long (~100 Myr) bursts of star formation (Iglesias-Páramo et al. 2004)
  - Metallicity: would lead to a *larger* Hα-to-FUV ratios at low metallicity, producing an effect that is the opposite of what is observed

Porosity of the ISM

- Shell morphology favours the existence of low-density areas with holes where the ionising photons can escape ==> the difference in log [SFR(Hα)/SFR(FUV)] could be due to leakage of ionising photons, implying f_{esc} ~0-25%

- Other explanations for the observed SFR(Hα)/SFR(FUV) behaviour:
  - Absorption of LyC photons by the dust inside the regions (Inoue 2001): shells would have higher fractions of dust than compact regions (this is not observed, Verley et al. 2010)
  - Non-constant SFR: to explain the observed trends very intense (a factor of 100) and very long (~100 Myr) bursts of star formation (Iglesias-Páramo et al. 2004)
  - Metallicity: would lead to a *larger* Hα-to-FUV ratios at low metallicity, producing an effect that is the opposite of what is observed
  - Stochastic IMF effects and/or IMF variations seem to reproduce well the observations (e.g. Pflamm-Alternburg et al. 2009)

Porosity of the ISM

- Shell morphology favours the existence of low-density areas with holes where the ionising photons can escape ==> the difference in log [SFR(Hα)/SFR(FUV)] could be due to leakage of ionising photons, implying f_{esc} ~0-25%

- Other explanations for the observed SFR(Hα)/SFR(FUV) behaviour:
  - Absorption of LyC photons by the dust inside the regions (Inoue 2001): shells would have higher fractions of dust than compact regions (this is not observed, Verley et al. 2010)
  - Non-constant SFR: to explain the observed trends very intense (a factor of 100) and very long (~100 Myr) bursts of star formation (Iglesias-Páramo et al. 2004)
  - Metallicity: would lead to a *larger* Hα-to-FUV ratios at low metallicity, producing an effect that is the opposite of what is observed
  - Stochastic IMF effects and/or IMF variations seem to reproduce well the observations (e.g. Pflamm-Alternburg et al. 2009)

Leakage, in combination with other possible mechanisms, might explain the differences in the SFR(Hα)/SFR(FUV) for star-forming objects.

Conclusions

The escape fraction of ionising radiation from HII regions can be up to ~50%, but an accurate quantification of this quantity is difficult to estimate.

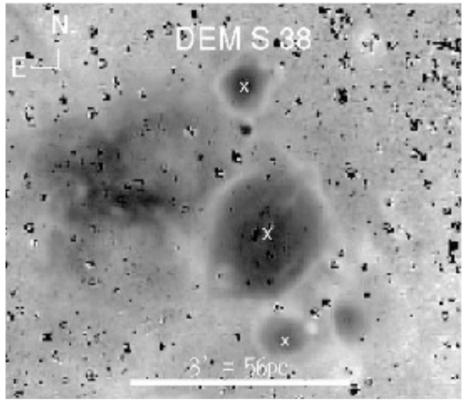

Emission line ratios involving low degree of ionisation can give clues if the regions are density or ionisation bounded: IPM is a very promising method to predict the status of the HII regions

SFR derived from Hα and FUV are consistent for galaxies with SFR > 1 $M_\odot$ yr^{-1}. However, Hα emission tends to underpredict the SFR relative to the prediction of FUV emission in low-luminosity dwarf galaxies

Leakage of ionising photons can affect the SFR estimation of the low mass galaxies and can partially explain the discrepancy between the SFR derived from Hα and from FUV.

TABLE 2

PHOTOIONIZATION MODELS BASED ON A SET OF ATMOSPHERES WITH $Z_* = 0.2Z_\odot$

	REGION		MODEL						
LINE RATIOS[a]	A	3 and 13	L.1	L.2	L.3	L.4	L.5	L.6	L.7
[O III] $I(\lambda\ 5007)$/[O II] $I(\lambda 3727)$	0.738	0.750	1.633	0.492	0.383	0.595	0.597	0.578	0.769
[S III] $I(\lambda 6312)$/[S II] $I(\lambda 6725)$	−0.857	−0.744	−0.004	−0.883	−0.974	−0.802	−0.847	−0.776	−0.659
[Ar IV] $I(\lambda 4740)$/[Ar III] $I(\lambda 7135)$......	−1.111	−1.392	−0.614	−1.233	−1.292	−1.179	−1.214	−1.155	−1.136
[O III] $I(\lambda 4363)/I(\lambda 5007)$................	−1.854	−1.915	−2.041	−2.015	−2.010	−2.021	−2.100	−1.951	−2.018
He II $I(\lambda 4686)$ /He I $I(\lambda 4471)$...........	−1.155	−1.430	−0.905	−1.286	−1.337	−1.242	−1.243	−1.243	−3.209
[S II] $I(\lambda\ 6716)/I(\lambda 6731)$	0.144	0.142	0.152	0.116	0.106	0.124	0.124	0.123	0.123
[S II] $I(\lambda\ 4069 + 4076)/I(\lambda 6725)$	−1.115	−0.940	−1.104	−1.050	−1.038	−1.060	−1.086	−1.037	−1.060
[O III] $I(\lambda 5007)/I(\mathrm{H}\beta)$..................	0.735	0.710	0.625	0.541	0.518	0.559	0.579	0.526	0.609
[O II] $I(\lambda 3727)/I(\mathrm{H}\beta)$	−0.003	−0.040	−1.008	0.049	0.135	−0.036	−0.018	−0.052	−0.160
He II $I(\lambda 4686)$ $/I(\mathrm{H}\beta)$..................	−2.571	−2.844	−2.419	−2.804	−2.856	−2.759	−2.753	−2.766	−4.708
$L(\mathrm{H}\alpha)$ (dex)...............................	...	...	38.987	38.978	38.987	38.977	38.988	38.981	38.989
N_e (rms) (cm^{-3})	...	...	9.00	9.00	9.00	9.00	9.00	9.00	9.00
Radius (10^{20} cm)	...	...	2.00	2.01	2.01	2.01	2.00	2.04	2.02
N_e (local)	...	...	9.00	100	130	80	80	80	...
ϵ..	...	...	1.00	0.0081	0.005	0.0127	0.0127	0.0127	0.013
[O][b]	...	...	8.11	8.11	8.11	8.11	8.21	8.01	8.11
T_e(rad) (K)...............................	...	...	11200	11400	11500	11400	10700	12000	11400
T_e(vol) (K)	...	...	10800	11200	11300	11100	10600	11700	11100
T_e ([O III]) (K)	13070	12430	10800	11300	11300	11200	10600	11800	11200

[a] Given by log $I(\lambda_1)/I(\lambda_2)$.

[b] Gaseous abundances given by $12 + \log N(\mathrm{O})/N(\mathrm{H})$.